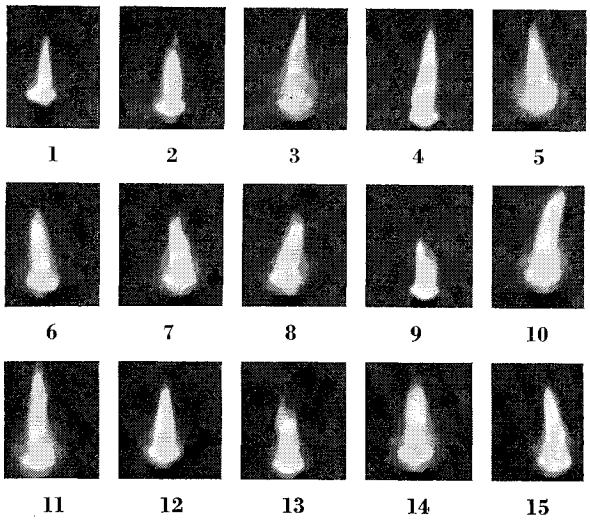

Fig. 4 High-speed Fastax pictures from a nitrogen plasmajet, F-40 plasma torch: I = 260 amp, P = 1 atm, flow rate = 150 scfh.

cylindrical or nozzle-shaped anodes of plasma generators. From a number of high-speed Fastax movies taken simultaneously with the voltage fluctuations, the characteristic behavior of the fluctuating mode of the arc could be established.[1]

In order to make sure that the geometry, which is of course quite different in this case, is not an important factor for the origin of such fluctuations, the same type of fluctuations in the F-40 plasma torch were generated by using nitrogen as working fluid. The results are shown in Figs. 3 and 4. The saw-tooth shape of the voltage fluctuations together with the high amplitude of about 50 v, which is almost half of the maximum arc voltage, indicate already the typical features of a restriking arc. Restriking occurs with a frequency of about 5 kc. In addition to these findings, Fastax high-speed pictures taken from the nitrogen plasmajet (Fig. 4) indicate irregularities in the plasmajet. From these investigations it may be concluded that the temperature measurements usually reported for argon jets at moderate gas flow rates[6] represent really steady-state temperatures rather than time-averaged values.

References

[1] Pfender, E., Wutzke, S. A., and Eckert, E. R. G., "An arc tunnel facility for the thermal analysis of anode and cathode regimes in an electric arc column," Heat Transfer Lab., TR-58, Univ. of Minnesota (1964); also NASA CR-54080 (1964).

[2] Dooley, M. T., McGregor, W. K., and Brewer, L. E., "Characteristics of the arc in a Gerdien-type plasma generator," Arnold Engineering Development Center AEDC-TR-61-13 (1961).

[3] Wheaton, T. R. and Dean, R. C., Jr., "On anode gas-sheath electrical breakdown in a high-pressure-arc plasma generator," Research Report, Thayer School of Engineering, Dartmouth College, Hanover, N. H. (November 1961).

[4] Krülle, G., "Motion of the plasma column in the interior and at the exit of an arc jet," *Proceedings of Specialist Meeting, Arc Heaters and MHD Accelerators for Aerodynamic Purposes, AGARD Fluid Dynamics Institute* (Technical Editing Reproduction Ltd. Hartford House, London, 1964.

[5] Brückner, R., "Spektroskopische Temperaturmessungen oberhalb 3500°C und Bestimmung der Temperaturverteilung eines Plasmabrenners bei Atmosphärendruck," Ber. Deut. Keram. Ges. **40**, 603–614 (1963).

[6] Cremers, C. J. and Pfender, E., "Thermal characteristics of a high and low mass flux argon plasma jet," Heat Tranfers Lab., TR-57, Univ. of Minnesota (1964); also Aeronautical Research Lab. Rept. 64-191 (1964).

Motion of Re-Entry Vehicles during Constant-Altitude Glide

H. E. WANG*
Aerospace Corporation, El Segundo, Calif.

DURING re-entry into earth atmosphere, a vehicle can often be "flown" at a constant altitude by rolling about its velocity vector at a fixed angle of attack. Such a maneuver produces lateral range and also eliminates trajectory oscillation. The lateral range obtained during such a flight has been computed numerically and is presented in Ref. 1 and discussed in Ref. 2. This note, however, presents analytic solutions. For a re-entry vehicle "flying" at a constant altitude, the applicable equations of motion are

$$(2W/C_DA\rho)(dV/dt) = -gV^2 \tag{1}$$

$$V^2(L/D)\cos\varphi = (2W/C_DA\rho)[1 - (V/V_s)^2] \tag{2}$$

$$\frac{d\psi}{dt} = \left(\frac{L}{D}\right)\frac{Vg\sin\varphi}{(2W/C_DA\rho)} - \frac{Vg\cos\psi\tan\lambda}{V_s^2} \tag{3}$$

and the kinematic equations are

$$d\lambda/dt = Vg\sin\psi/V_s^2 \tag{4}$$

$$d\mu/dt = Vg\cos\psi/(V_s^2\cos\lambda) \tag{5}$$

The symbol φ is the bank angle measured from the local vertical, ψ is the turn angle measured from the vehicle's original heading, λ is the ratio of the lateral range (measured from the original great circle) to the radius of the earth, μ is the ratio of the down range (measured from the beginning of the glide) to the radius of the earth, and V_s is the orbital speed at sea level. The variation of the gravitational acceleration with altitude has been neglected. Other symbols have their usual meaning. Defining

$$C = 2W/(C_LA\rho\,V_s^2) \tag{6}$$

and eliminating Eq. (1), we obtain

$$-V(d\psi/dV) = (L/D)(\sin\varphi - C\cos\psi\tan\lambda) \tag{7}$$

$$-V(d\lambda/dV) = (L/D)(C\sin\psi) \tag{8}$$

$$-V(d\mu/dV) = (L/D)(C\cos\psi/\cos\lambda) \tag{9}$$

These equations can be solved analytically if $\sin\varphi = 1$ is assumed. This approximation has been thoroughly studied

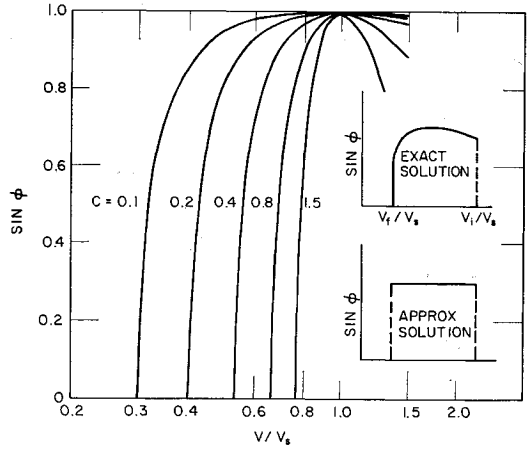

Fig. 1 Variation of $\sin\varphi$ as a function of V/V_s and C.

Received February 10, 1965; revision received April 15, 1965.
* Manager, Aerophysics Section, Applied Mechanics Division. Member AIAA.

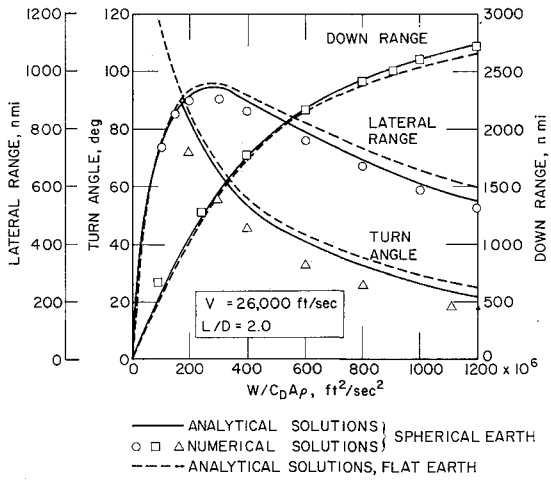

Fig. 2 Comparison of analytical solution with numerical solution.

in Ref. 3, and it suffices to examine Fig. 1 to see that the approximation is reasonably accurate. Figure 1 is a plot of Eq. (2) in terms of $\sin\varphi$.

There was an approximated model considered in Ref. 2, namely, the "flat-earth" approximation in which the lateral centrifugal force term $Vg\cos\psi\tan\lambda/V_s^2$ was omitted from Eq. (3). The "flat-earth" approximation has been shown in Ref. 2 to be acceptable for low values of C regardless of the magnitude of lateral range and initial velocity when compared with the spherical earth solutions. The solutions of the "flat-earth" model together with the approximations $\sin\varphi = 1$ and small λ can be readily obtained by integrating Eqs. (7–9). They are

$$\psi_0 = (L/D)\ln(V_i/V) \tag{10}$$

$$\lambda_0 = C(1 - \cos\psi_0) \tag{11}$$

$$\mu_0 = C\sin\psi_0 \tag{12}$$

Here the subscript 0 indicates the "flat-earth" approximation, and i indicates the initial condition. These approximate solutions have been shown in Ref. 3 to agree extremely well with numerical solutions that do not assume $\sin\varphi = 1$. A sample of the calculation is shown in Fig. 2 together with the spherical earth solutions, which will be discussed later.

One interesting observation can be made of the "flat earth" solution. Combining Eqs. (11) and (12), one gets

$$(\lambda_0 - C)^2 + \mu_0^2 = C^2 \tag{13}$$

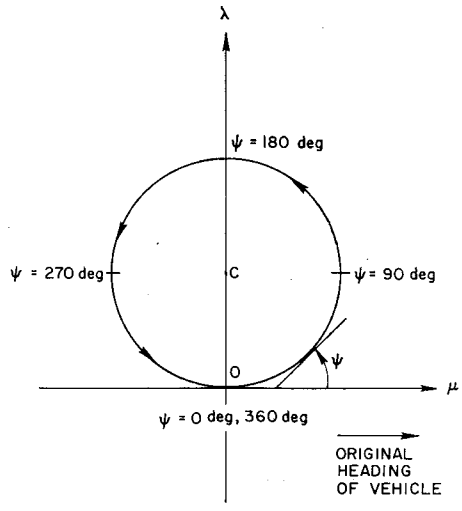

Fig. 3 Vehicle flight path at very small C.

This equation represents a circle with its center at $\lambda_0 = C$ and its radius equal to C. This shows that the vehicle, while making a constant-altitude turn, describes a circular path. Depending on the aerodynamics, the mass characteristics, and the altitude, the vehicle may find itself anywhere along the circumference of the circle by the time it reaches equilibrium glide. As indicated in Fig. 3, the vehicle could make a 180° turn in which case it would have acquired a lateral displacement of $2C$ with no net forward displacement by the time it reaches the equilibrium glide line. From that moment on, the vehicle would fly in the direction opposite to its original heading. In fact, the vehicle could make a full 360° turn and find itself back to the original location at a much lower velocity. For a vehicle with $L/D = 2$, $W/C_LA = 25$ psf, and $V_i = 32{,}000$ fps, the 180° turn must be performed at an altitude of 184,000 ft whereas the 360° turn requires 104,000 ft. The radius of the turn is 242 and 9.7 naut miles, and the final velocity is 6650 and 1380 fps, respectively. The aerodynamic loading and heating would be prohibitive in these cases.

The full solutions to Eqs. (7–9) including the lateral centrifugal force term (called spherical earth solutions) were obtained in Ref. 3 by the method of perturbation, since the spherical earth correction was not large for the normal range of $W/C_DA\rho$ as indicated in Ref. 2. The approximation $\sin\varphi = 1$ remained. In reviewing the results of Ref. 3, however, Levin[4] suggested a closed-form solution in which the only approximation was $\sin\varphi = 1$. Since the closed-form solutions are mathematically neater, they are illustrated below. We combine Eqs. (7) and (8) and get

$$(1 - C\cos\psi\tan\lambda)d\lambda/d\psi = \sin\psi \tag{14}$$

or

$$d(C\cos\psi\cos\lambda)/d\lambda = -\cos\lambda \tag{15}$$

Thus,

$$\sin\lambda = C(1 - \cos\psi\cos\lambda) \tag{16}$$

or

$$\sin\lambda = C\left\{\frac{1 - \cos\psi(1 - C^2\sin^2\psi)^{1/2}}{1 + C^2\cos^2\psi}\right\} \tag{17}$$

The solutions for μ and ψ are given by

$$\sin\mu = C\sin\psi \tag{18}$$

$$\cos\psi = \frac{\cos\eta + C^2}{[(1 + C^2)^2 - 4C^2\sin^4(\eta/2)]^{1/2}} \tag{19}$$

where

$$\eta = (L/D)(1 + C^2)^{1/2}\ln(V/V_i) \tag{20}$$

It can be readily shown that, for small values of C, these spherical earth solutions degenerate to the "flat-earth" solutions. The accuracy of Eqs. (17–19) is extremely high when compared with numerical solutions as shown in Fig. 2. In Fig. 2, a nonrotating earth is assumed, and the constant-altitude glide ends at the equilibrium glide line; thus, the final velocity is given by

$$V_f = V_s/[1 + (1/C)]^{1/2} \tag{21}$$

It is also seen in Fig. 2 that the approximate "flat-earth" solutions do not deviate too much from the approximate spherical earth solutions. For preliminary design work, the simple "flat earth" solutions are often sufficient.

The sample calculations presented in this note are for $L/D = 2$ and $V_i = 26{,}000$ fps. The analytic solutions for both earth models have been shown in Ref. 3 to be sufficiently accurate for other values of L/D and V_i. Thus, one is led to conclude that the motion of a re-entry vehicle "flying" at a constant altitude at a banked attitude can be accurately described with the approximation $\sin\varphi = 1$.

References

[1] Shulsky, R. S., "Study of a particular lateral-range re-entry maneuver," TM1364-61-16, Martin Co., Denver, Colo. (August 1961).

[2] Wang, H. E. and Skulsky, R. S., "Characteristics of lateral range during constant-altitude glide," AIAA J. 1, 703–704 (1963).

[3] Wang, H. E., "Approximate solutions of the lateral motion of re-entry vehicles during constant altitude glide," Aerospace Corp. TDR-169(3560-10)TN-1 (February 1963).

[4] Levin, E., private communication, Aerospace Corp. (July 1963).

Wave Motion in a Radiating Simple Dissociating Gas

INGE L. RYHMING*

Aerospace Corporation, El Segundo, Calif.

IN this note, some theoretical results regarding the coupled effects of relaxation and radiation on the wave propagation in a simple dissociating gas are summarized. The results are derived using the quasi-equilibrium theory of radiation, taking into consideration some details of the physics of the thermal radiation in an oxygen-like gas, consisting of molecules and atoms only (no ionization). A detailed discussion of the theory is given in Ref. 1.

The equations of motion for the inviscid, one-dimensional, time-dependent flow are taken as

Continuity

$$\rho_t + u\rho_x + \rho u_x = 0 \tag{1}$$

Momentum

$$\rho u_t + \rho u u_x + p_x = 0 \tag{2}$$

Energy

$$\rho h_t + \rho u h_x - p_t - u p_x = Q(\rho, \alpha, T) \equiv A_{\text{tot}} - E_{\text{tot}} \tag{3}$$

Rate

$$\alpha_t + u\alpha_x = \theta^{-1} L(p, \rho, \alpha) \tag{4}$$

in which equations the radiation pressure, the contribution to internal energy by radiation, and the effect of photodissociation are neglected. Furthermore, in the equations, ρ, u, p, h, α, and T have their usual meaning ($T \equiv$ translational temperature), Q is the heat input due to emission and absorption of radiation, and the particular form of the right-hand side of Eq. (4) is adopted after the work by Vincenti.[2] With p, ρ, and α chosen as primary state variables, the equations of state are expressed as $T = T(p, \rho, \alpha)$ and $h = h(p, \rho, \alpha)$.

The Q function in Eq. (3) needs some consideration. We assume that the simple dissociating gas is oxygen-like, such that the gas has a strong and continuous absorption in the UV part of the spectrum (Schumann-Runge), and that this spectrum is the most important contributor to the radiation in the gas. Using the quasi-equilibrium theory of radiation,[3] the total rate of emission E_{tot} is consequently taken as

$$E_{\text{tot}} = 4\pi(1 - \alpha)\rho\rho_N^{-1} \int_{\nu_1}^{\nu_2} \kappa_\nu(T) B_\nu(T) d\nu \tag{5}$$

where $\kappa_\nu(T)$ is the absorption coefficient of the continuum, and $B_\nu(T)$ is the Planck function; the factor $\rho\rho_N^{-1}$ comes from Beer's law (ρ_N is the standard density), the factor $(1 - \alpha)$ is due to the dissociation process in the gas, and ν_1 and ν_2 are the beginning and end of the continuum spectrum, respectively. However, $\kappa_\nu(T)$ varies weakly with frequency at temperatures of interest and can be regarded as independent of ν in the pertinent frequency region. Because of this, and to facilitate a simple calculation of A_{tot} in Eq. (3), a frequency independent absorption coefficient κ of the continuum is defined in terms of a Planck mean

$$\kappa = (1 - \alpha)\rho\rho_N^{-1} \int_{\nu_1}^{\nu_2} \kappa_\nu(T) B_\nu(T) d\nu \Big/ \int_{\nu_1}^{\nu_2} B_\nu(T) d\nu \tag{6}$$

Using this value of κ for the continuum, we define next an optical thickness ξ by

$$\xi = \kappa_0^{-1} \int_0^x \kappa(x') dx' \qquad \nu_1 < \nu < \nu_2 \tag{7}$$

where κ_0 is some fixed value of κ. With the help of this variable, it is possible to express A_{tot} in a simple integral form. When no solid surfaces are present, the combined result for A_{tot} and E_{tot} gives the following expression for Q:

$$Q = 4\pi\kappa \left[\int_{-\infty}^{+\infty} G(T) E_1(\kappa_0 |\xi - \xi'|) d\xi' - 2G(T) \right] \tag{8}$$

where

$$2G(T) = \int_{\nu_1}^{\nu_2} B_\nu(T) d\nu$$

and where $E_1(z)$ is a particular form of the integro-exponential function $E_n(z)$ of the general order n (for definition see Ref. 3, p. 253). For a quantitative determination of the radiative properties, a particularly suitable representation of $\kappa_\nu(T)$ for the present purposes has been given by Sulzer and Wieland.[4]

We assume next that acoustic waves are created harmonically at the origin by some unspecified means. The acoustic approximations to the basic equations are obtained, as usual, by linearization, and we write $h = h_0 + h'$, $\kappa = \kappa_0 + \kappa'$, $u = u'$, etc., where the subscript 0 denotes the uniform conditions in the undisturbed gas, and the primes denote small deviations therefrom. The linearized equations can be reduced to a single equation by introducing a potential function Φ, satisfying identically the linearized momentum equation, i.e.,

$$u' = \Phi_x \qquad p' = -\rho_0 \Phi_t \tag{9}$$

with the result that

$$\frac{\partial W_S(\Phi)}{\partial t} = 8 \frac{\kappa_0 a_{f_0}}{Bo} \times \int_{-\infty}^{+\infty} \operatorname{sgn}(x' - x) E_2(\kappa_0 |x - x'|) \frac{\partial W_T(\Phi)}{\partial x'} dx' \tag{10}$$

where

$$W_S = K_S \frac{\partial}{\partial t} \left(\frac{\partial^2}{\partial x^2} - \frac{1}{a_{f_0}^2} \frac{\partial^2}{\partial t^2} \right) + \frac{\partial^2}{\partial x^2} - \frac{1}{a_{e_0}^2} \frac{\partial^2}{\partial t^2} \tag{11}$$

$$W_T = K_T \frac{\partial}{\partial t} \left(\frac{\partial^2}{\partial x'^2} - \frac{1}{c_{f_0}^2} \frac{\partial^2}{\partial t^2} \right) + \frac{\partial^2}{\partial x'^2} - \frac{1}{c_{e_0}^2} \frac{\partial^2}{\partial^2 t} \tag{12}$$

Here a_{f_0} and a_{e_0} are the frozen and equilibrium *isentropic* speeds of sound, respectively, and c_{f_0} and c_{e_0} are the frozen and equilibrium *isothermal* speeds of sound, respectively. Furthermore, K_S and K_T are related to the relaxation time in the gas, such that in an equilibrium flow (infinite reaction rate) K_S and K_T approach zero, whereas in a frozen flow (zero reaction rate) K_S and K_T approach infinity. Another important parameter in Eq. (10) is the Boltzmann number Bo. It is defined as

$$Bo = \bar{c}_{p_0} \rho_0 a_{f_0} / (\pi/2)(dG/dT)_{T=T_0} \tag{13}$$

Received February 5, 1965. This work was supported by the U. S. Air Force under Contract No. AF 04(695)-269.

* Member of the Technical Staff, Aerophysics Department, Aerodynamics and Propulsion Research Laboratory. Member AIAA.